ESA UNCLASSIFIED – For Official Use

estec

European Space Research
and Technology Centre
Keplerlaan 1
2201 AZ Noordwijk
The Netherlands
T +31 (0)71 565 6565
F +31 (0)71 565 6040
www.esa.int

DOCUMENT

SEE test of the Intersil Quad CMOS Driver ISL7457SRHF, RADEF November 2014

Prepared by	**Véronique Ferlet-Cavrois**
Reference	**ESA-TECQEC-LAB-TR-0758**
Issue	**1**
Revision	**2**
Date of Issue	**26/08/2015**
Status	**Authorised**
Document Type	**RP**
Distribution	

European Space Agency
Agence spatiale européenne

APPROVAL

Title SEE test of the SSDI SFR130 power MOSFET with the microprobe at GSI, Darmstadt, May 2014	
Issue 1	**Revision** 2
Author Véronique Ferlet-Cavrois	**Date** 26/08/2015
Approved by	**Date**

CHANGE LOG

Reason for change	Issue	Revision	Date

CHANGE RECORD

Issue 1	Revision 2		
Reason for change	**Date**	**Pages**	**Paragraph(s)**

Table of contents:

1 INTRODUCTION 4
2 APPLICABLE AND REFERENCE DOCUMENTS 4
2.1 Applicable documents 4
2.2 Reference documents 4
3 ACRONYMS 5
4 TESTED DEVICES 6
5 TEST FACILITY 7
6 TEST CONDITIONS 8
7 TEST RESULTS 9
8 CONCLUSION 18
9 APPENDIX 1: IRRADIATION TEST RUNS 19
10 APPENDIX 2: MICROSCOPE VIEW OF THE FAILURE SPOT 22

1 INTRODUCTION

The following document describes the SEE (single event effect) test of the Intersil non-inverting, quad CMOS Driver ISL7457SRHF [RD1, RD2] with heavy ion broad beam at RADEF, Jyväskylä, Finland [RD3-RD4]. This experiment was undertaken to assess the worst-case SEE test conditions and the SEE sensitivity of this device.

The tested parts are prototypes ISL7457SRHF/PROTO samples from Intersil. They are not space grade samples. For project specific application it is recommended to SEE test each flight-lot of the ISL7457SRHF according to [AD1].

The experiment was performed by Michele Muschitiello and Véronique Ferlet-Cavrois (TEC-QEC), funded by ESA Technical Assessment budget and the CHEOPS mission.

2 APPLICABLE AND REFERENCE DOCUMENTS

2.1 Applicable documents

[AD1] ESCC25100, "Single Event Effect Test Method and Guidelines", Oct. 2014.

2.2 Reference documents

[RD1] ISL7457SRHF datasheet, Intersil

[RD2] "SEE Testing of the ISL7457SRH Non-Inverting, Quad CMOS Driver", Sept. 2009, available on Intersil web site

[RD3] A. Virtanen, R. Harboe-Sorensen, A. Javanainen, H. Kettunen, H. Koivisto, I. Riihimaki, "Upgrades for the RADEF Facility," IEEE Radiation Effects Data Workshop, pp. 38-41, July 2007.

[RD4] RADEF facility, Jyväskylä, Finland https://www.jyu.fi/fysiikka/en/research/accelerator/radef/

[RD5] J. R. Schwank, M. R. Shaneyfelt, J. A. Felix, P. E. Dodd, J. Baggio, V. Ferlet-Cavrois, P. Paillet, G. L. Hash, R. S. Flores, L. W. Massengill, E. Blackmore, "Effects of Total Dose Irradiation on Single-Event Upset Hardness," IEEE Trans. Nuc. Sci. vol. 53, no. 4, Aug. 2006.

[RD6] EADS Astrium report prepared by Renaud Gougerat, "Failure analysis of EL7457 for GAIA project," TEC.FR.07.NT.2043, Iss. 0, Rev. 0, dated 14 March 2007.

[RD7] Hugh D. R. Evans, "CHEOPS FEE Reliability - ISL7457SRH SEE Analysis," ESA Memo ref. ESA/TEC-EES/2014.108/HE, dated 02 Apr. 2015

3 ACRONYMS

SEE Single Event effects
SET Single Event Transients
SEB Single Event Burnout
RADEF Radiation Effects Facility

4 TESTED DEVICES

The tested device were the ISL7457SRH/PROTO in a 16 Ld ceramic flatpack package. Five samples were de-lidded to expose the die for heavy ion tests. Table 1 summarises the characteristics of the tested devices. Figure 1 shows a picture of a de-lidded sample.

Manufacturer	Reference	Function	Package	Internal reference
Intersil	ISL7457SRH /PROTO	non-inverting, quad CMOS Driver	16 Ld ceramic flatpack	Five samples, From s1 to s5

Table 1: Details of the tested devices

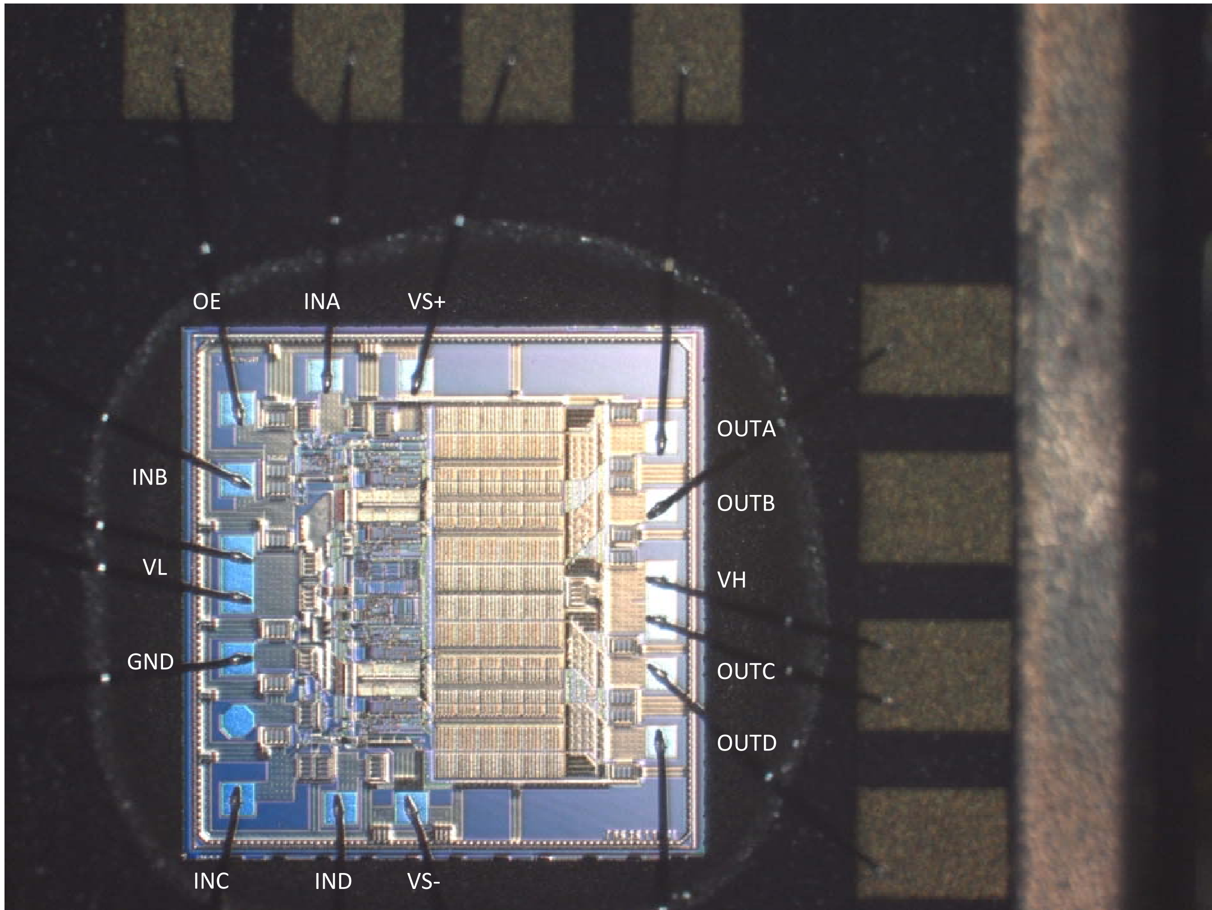

Figure 1: Picture of the die. The die dimensions are 2390µm x 2445µm [RD1].

5 TEST FACILITY

The experiment was performed at RADEF in static bias condition at room temperature and under vacuum [RD3, RD4].
Krypton and Xenon ion beams were used during the experiment (Fig. 2).

Experimenters: Michele Muschitiello, Véronique Ferlet-Cavrois (TEC-QEC)

Facility: RADEF, Jyväskylä, Finland [RD3]

Operators : Heikki Kettunen, Mikko Rossi (RADEF)

Cocktail 9.3 MeV/nucleon, test in vacuum, wobbler on, no diffusion foil.

Date: 12-13 November 2014

Ions: Kr 768MeV, in silicon: range 94µm, LET 32.1MeVcm²/mg

Xe 1217 MeV, in silicon: range 89um, LET 60 MeVcm²/mg

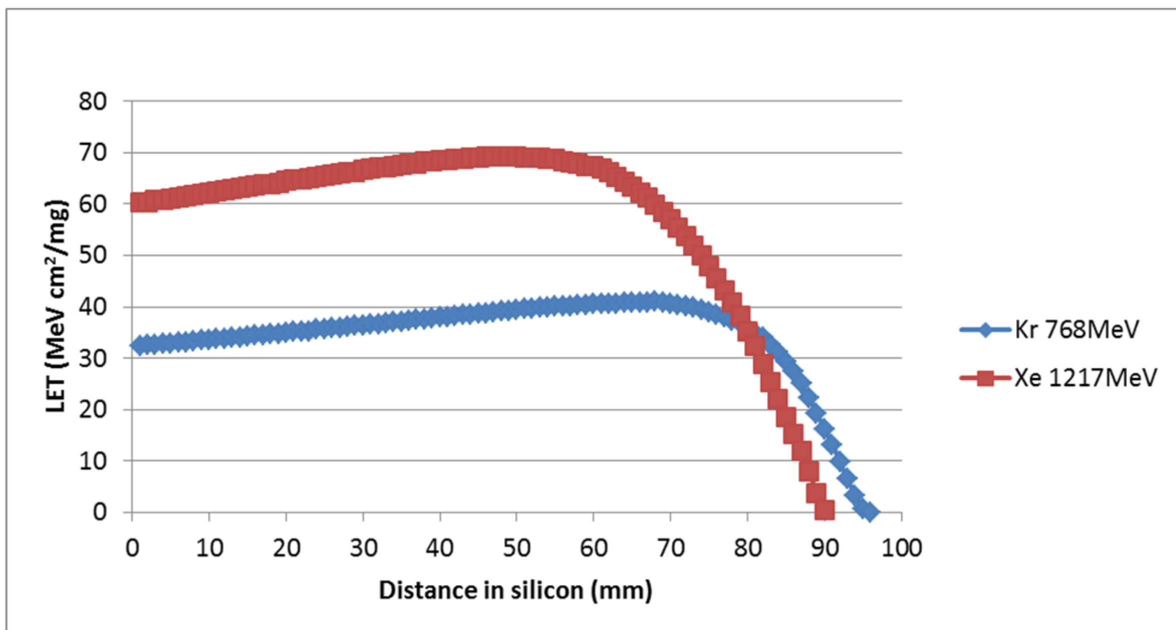

Figure 2: LET vs. range in silicon for Kr and Xe used at RADEF during this experiment.

6 TEST CONDITIONS

The ISL7457/PROTO devices were biased in the same conditions as those used in the Intersil SEE test report [RD2]:

- VS- was grounded
- VS+ (called VS below) and VH were biased at the same voltage, but on separate supply channels, so that VS and VH supply currents were monitored separately, respectively on Channel A and Channel B of the Keithley power supply 2612A.
  - VH supplied the output stages of the DUT (right side of the die in Fig. 1)
  - VS supplied the inputs and circuitry (left side of the die in Fig. 1)
- Inputs INA and INB were tied to VS through 10kΩ,
  - outputs OUTA and OUTB were normally high, tied to VH through 1kΩ
- Inputs INC and IND were tied to ground through 10kΩ,
  - outputs OUTC and OUTD were normally low, tied to ground through 1kΩ

The Fig. 3 below shows the SEE test set-up. The single event transients (SETs) on VS and VH were detected with Tektronix current probes (CT2 1mV/mA on VH and CT1 5mV/mA on VS). The probes were connected to two 50Ω input channels of a Yokogawa DLM2054 oscilloscope. The Yokogawa was set to detect transients on both channels (VS or VH) and to externally trigger a second oscilloscope, Agilent MSO9404A, which was registering transients from OUTA, OUTB, OUTC and OUTD on its four channels (with 1MΩ load input).

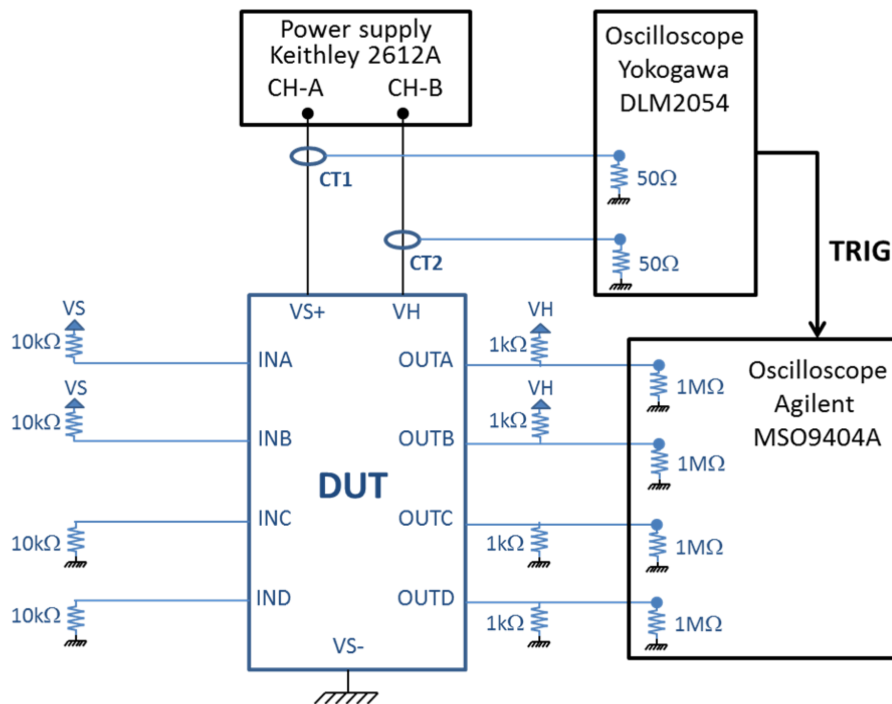

Figure 3: ISL7457 SEE test set-up.

7 TEST RESULTS

The irradiation run history is summarized in Appendix 1.

The five ISL7457/PROTO samples were irradiated successively, in the following order: s2, s1, s3, s4, s5.

Sample s2 was irradiated at 15 V with Xe ions at normal incidence. The device failed after exposure to a fluence of 5E5 Xe ions/cm². A sharp increase of the VH supply current was observed reaching the power supply current limit value of 10mA. No alteration of the VS supply current was observed. No visible failure site was observed under microscope on this sample. Transients and supply currents were not measured during this first run.

Sample s1 was irradiated with Kr ions at 15V. Different tilt and roll incident angles were employed in order to detect sensitivity to angling (see description of test runs in Appendix 1). No specific behaviour under tilt or roll angle was detected. The transients were correctly registered only from run4. Two distinct types of single event transients (SETs) were measured, either narrow or large, on the biased outputs, OUTA and OUTB, while no significant transients were measured on the grounded outputs, OUTC and OUTD. The histograms of the full width at half maximum of the SETs measured on OUTA of sample s1 during three runs are plotted in Fig. 4. The outputs OUTA and OUTB deliver similar histograms, with two distinct groups of transients, narrow (less than 20 µs) or large (between 60µs and 80µs). There are numerous narrow SETs, while there are only few large SETs.
Sample s1 failed at roll angle -60° during run8 at fluence 9E6 Kr ions/cm² after a cumulated dose of about 20 krad. The failure is characterised by a sharp increase of the VH supply current reaching the power supply current limit value of 10mA. Following optical inspection of s1, employing a microscope, the failure site appears to be located in the protection structure attached to the OUTB pad, presumably off-state (gate grounded) MOS transistor (see Appendix 2). The failure has a SEB (single event burnout) signature, with melting of the metal and insulating materials, because of large currents flowing in the low resistive failure spot.

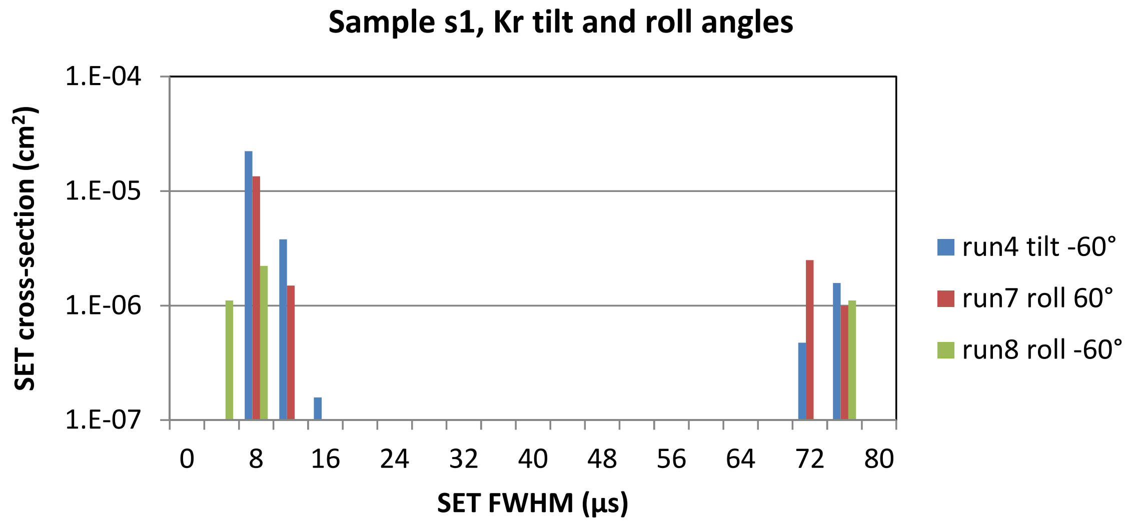

Figure 4: OUTA SET cross-section histogram of sample s1, as a function of the SET full width at half maximum (FWHM). Sample s1 was irradiated with Kr ions at different tilt and roll angles.

Sample s3 was irradiated with Kr ions at a roll angle of -60° at successively 12 V, 14 V and 15V supply bias. Again, two distinct types of transients were measured, either narrow or large, on the biased outputs, OUTA and OUTB, while no significant transients were measured on the grounded outputs, OUTC and OUTD. Fig. 5 show the histograms of the SET full width at half maximum measured on OUTA for runs 4-7-8. OUTB provides very similar histograms, with numerous narrow SETs and a few large SETs. Fig. 6a and Fig. 6b show examples of transients measured respectively on OUTA and OUTB during run 11 (VS = VH = 15 V). The transients #116 (black line) and #122 (green line) are examples of narrow transients, while transient #66 (blue line) is an example of large transient. Note that transients on the outputs (OUTA-B-C-D) are registered synchronously when a transient is detected on the VH or VS supplies. Interestingly, OUTA and OUTB displays the same type of transients. For example, the #66 OUTA and OUTB transients are both large transients, not perfectly identical, but very similar in width, amplitude and shape. The #116 and #122 OUTA and OUTB transients are both narrow and with very similar shape. Transient #123 has a particular shape: it corresponds to the device burn-out. OUTA and OUTB voltages saturate at about 12.5 V instead of 15 V. The burn-out reduced the impedance of the output stage to 1.25 kΩ (10 mA leakage current for 12.5 V bias), instead of 500 kΩ (about 30 µA leakage current for 15 V bias) in normal conditions. The burn-out is also revealed by a sharp increase of the VH supply current reaching the power supply current limit value of 10mA.. Under microscope the failure on sample s3 is located in the protection structure attached to OUTA (see Appendix 2).

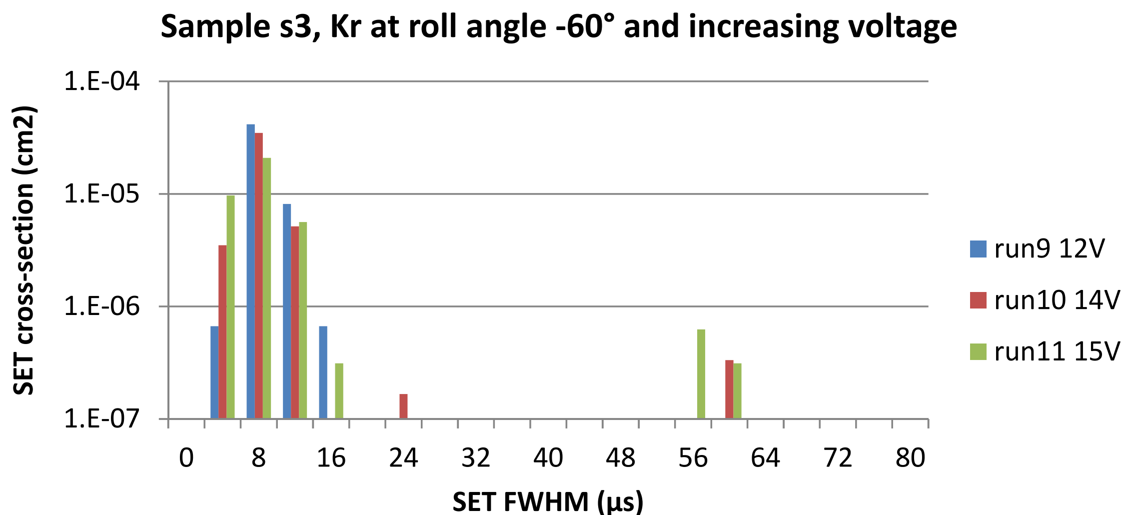

Figure 5: OUTA SET cross-section histogram of sample s3, as a function of the SET full width at half maximum (FWHM). Sample s3 was irradiated with Kr ions at -60° roll angle, and at increasing supply voltage (12 V, 14 V, 15 V).

a) Sample s3, run11, OUTA

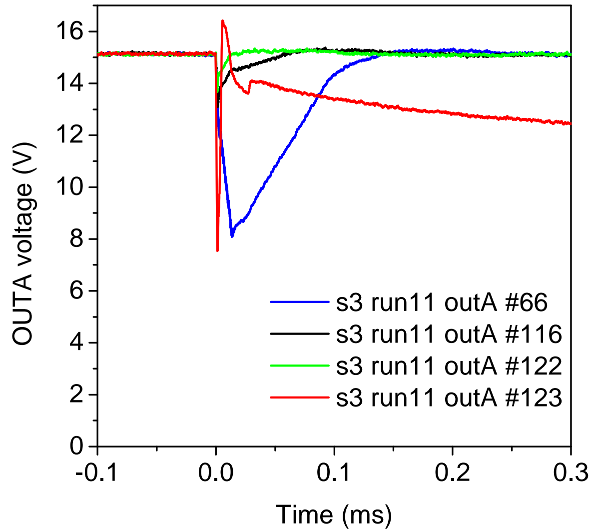

b) Sample s3, run11, OUTB

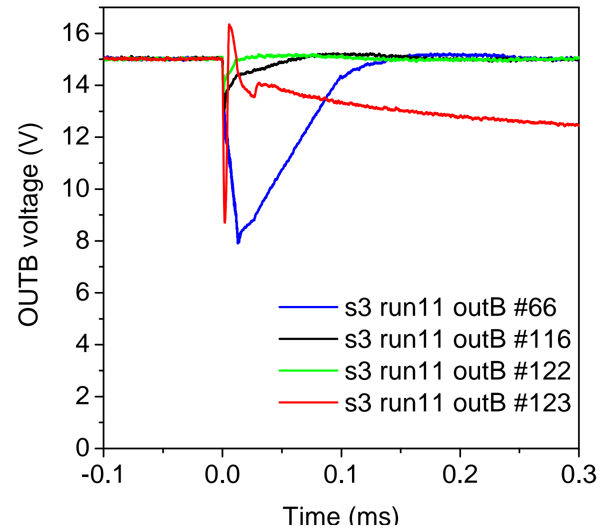

c) Sample s4, run15, OUTA

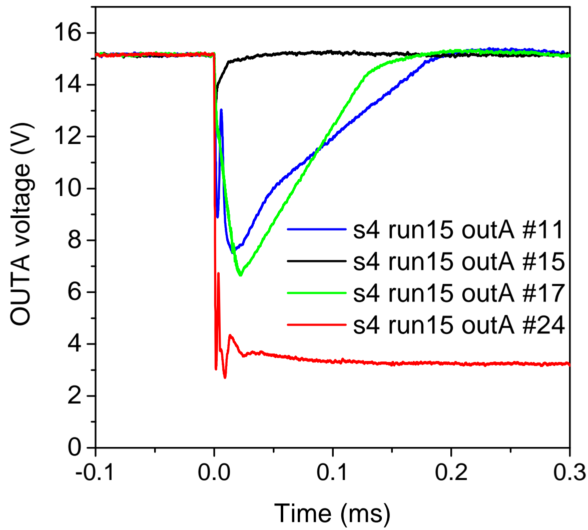

d) Sample s4, run15, OUTB

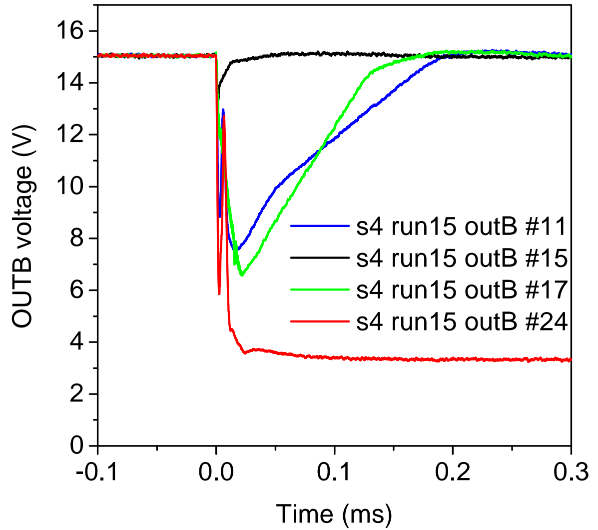

Figure 6: Examples of SETs measured on OUTA and OUTB of sample s3 and s4 biased at 15V (VS = VH = 15V), respectively under Kr (roll angle 60°) and Xe (normal incidence). The other outputs, OUTC and OUTD, were grounded and did not show significant transients.

Sample s4 was irradiated with Xe ions at normal incidence at successively 10 V, 12 V, 14 V, and 15 V. Fig. 7 shows the histogram of the OUTA SET full width at half maximum, with as before, two groups of SETs: one group of numerous narrow SETs and a second group of few large SETs. It seems that the width of the large SETs increases with the supply voltage. No definite conclusion may be drawn due to insufficient statistics.
Examples of narrow and large transients measured on OUTA and OUTB are shown in respectively Fig. 6c and Fig. 6d for run15 (VS = VH = 15 V). Transient #15 is a narrow transient, while transients #11 and #16 are large transients. At half maximum, large SETs are about 60-80µs, but the full width of the large SETs is at least twice larger, from 0.12 ms up to close to 0.2 ms. The last transient #24 shows the device burn-out, with VH voltage saturating at about 3 V after failure, instead of 15 V before failure. The burn-out reduced the impedance of the output stage to 0.3 kΩ, lower than for sample s3 (1.25 kΩ). It is believed that the cause of the burn-out is due to one of the large SETs.
VS and VH supply currents of sample s4 show the same failure signature as for all devices (Fig. 8): A sharp increase of the VH supply current was observed reaching the power supply current limit value of 10mA, while the VS supply current is barely affected, with only a slight decrease.

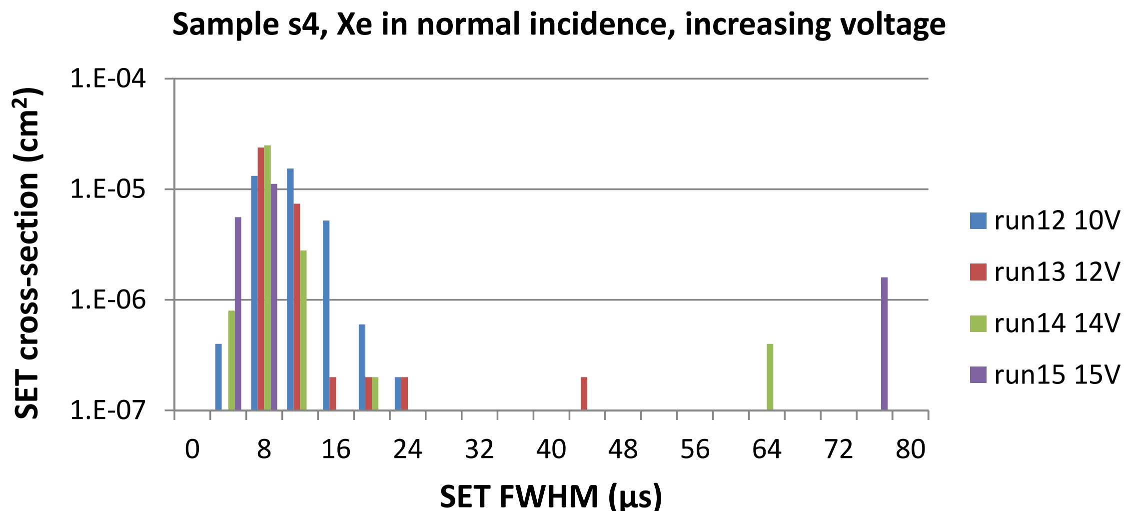

Figure 7: OUTA SET cross-section histogram of sample s4, as a function of the SET full width at half maximum (FWHM). Sample s4 was irradiated with Xe ions in normal incidence, and at increasing supply voltage (10 V, 12 V, 14 V, 15 V).

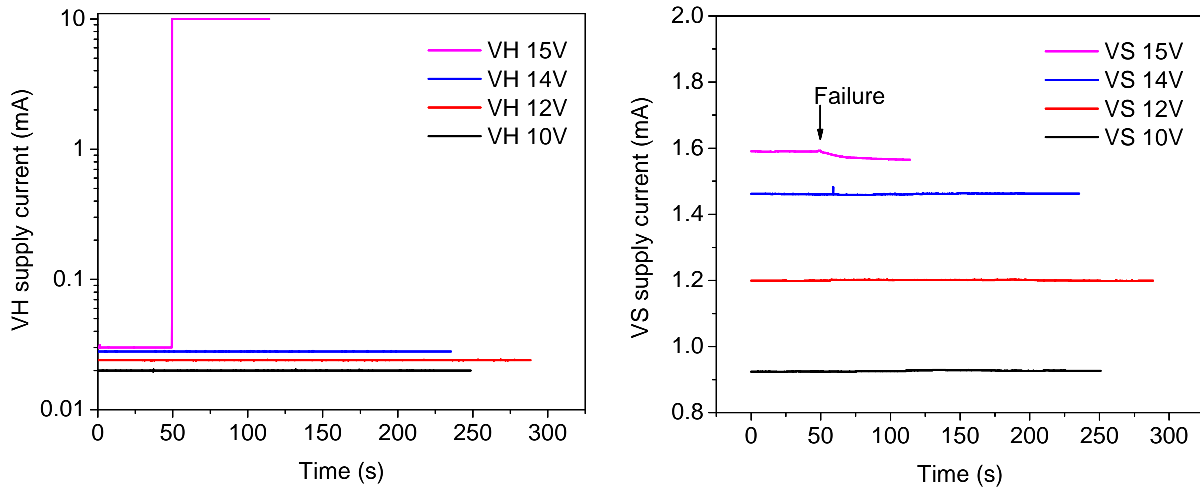

Figure 8: VH and VS supply currents during irradiation measured on sample s4. Note that the supply currents are continuously registered from about 20s when the device is biased before the irradiation starts, during irradiation, and until about 10s after irradiation.

Sample s5 was irradiated with Xe ions at normal incidence at successively 10 V, 12 V, 14 V, and 15 V. Fig. 9 shows the histogram of the OUTA SET full width at half maximum, with as before, two groups of SETs: one group of numerous narrow SETs and a second group of few large SETs. It seems again that the width of large SETs increases with the supply voltage, but the statistics of large SETs is low.
The cross-section of all SETs (narrow and large) and large SETs is plotted in Fig. 10, as a function of the device supply bias. The cross-section of large SETs increases exponentially with bias from 12 V. It is recommended that the ISL7457/PROTO is biased below 12 V to avoid large SETs and burn-outs. On the other hand, the cross-section of all SETs (narrow and large) is constant or even slightly decreasing.
The reason for the decreasing number of SETs is dose related, as shown in Fig. 11. The ISL7457/PROTO is particularly sensitive to total dose. It is advised to limit the cumulated dose to 10 krad for a conservative SEE test, relevant for a space application.
It should be noted that a similar behaviour, decrease of the SEE sensitivity with dose, has previously been observed in SRAMs [RD5], when the bias conditions (checkerboard pattern) during exposure and SEE measurement were identical. However, [RD5] also showed that if the bias condition during exposure and SEE measurement are opposite (checkerboard and reverse-checkerboard patterns), the SEE sensitivity increases. During our experiment, the ISL7457/PROTO was exposed and SET-SEB measured in the same static bias condition. It displayed a similar behaviour as the SRAMs in [RD5], i.e. decrease of the SEE sensitivity with dose when exposed and measured in the same bias conditions. However, in most applications, the ISL7457/PROTO is not used in static but for example as a CCD clock driver with a switching signal. It is believed that the dose effect on static SEE testing of this device is not representative to dynamic test conditions. If relevant, for example if the device is to be exposed to large doses during its lifetime in space, the SEE test should be performed in dynamic mode, identical to the application conditions. However, for missions with moderate dose exposure (< 10krad), the test in static is adequate with the condition that the exposure dose per sample is limited for a conservative SEE measurement.
Sample s5 failed at a fluence of 1E6 Xe ions/cm^2 and for a high supply voltage 15.5 V. The SEB voltage for this sample is higher than for the others (15 V), because it received the largest dose (25 krad). This illustrates the dose effect explained above.
Another interesting matter, see Fig. 10, is the cross-section value, which reveals a sensitive area. The cross-section of all SETs is 4E-5 cm^2 at maximum, i.e. a sensitive area of about 50×80 µm^2. Considering the die dimensions and the device picture in Fig. 1, the sensitive area of 50×80 µm^2 corresponds to the area of the protection structure attached to the OUTA and OUTB pads. As a matter of fact, the failure in sample s5 is located in the protection structure attached to OUTB (see Appendix 2).Contrary to the previous version of the device, the EL7457, where failures were located in the power MOSFETs [RD6], failures in the ISL7457 are visibly located in the protection structure for three samples (s1, s3, s5). For the other two samples (s2, s4), the failure spot is not visible, possibly too small (the current limitation reduces material melting). Comparing the EL7457 and ISL7457 pictures, it seems that the device has been redesigned and fabricated in a different technology, resulting in different failure modes.

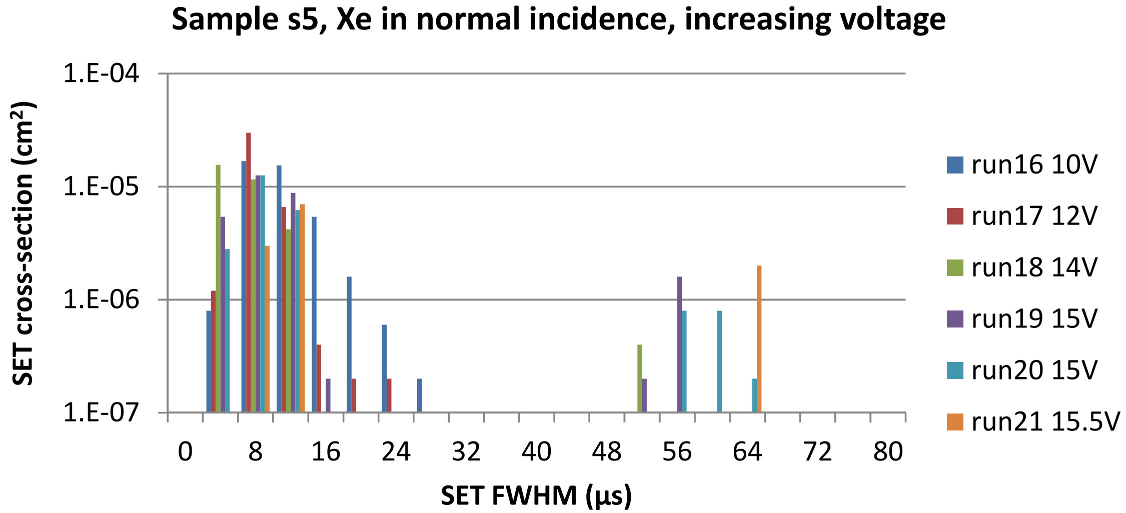

Figure 9: OUTA SET cross-section histogram of sample s5, as a function of the SET full width at half maximum (FWHM). Sample s5 was irradiated with Xe ions in normal incidence, and at increasing supply voltage (10 V, 12 V, 14 V, 15 V, 15 V, 15.5 V).

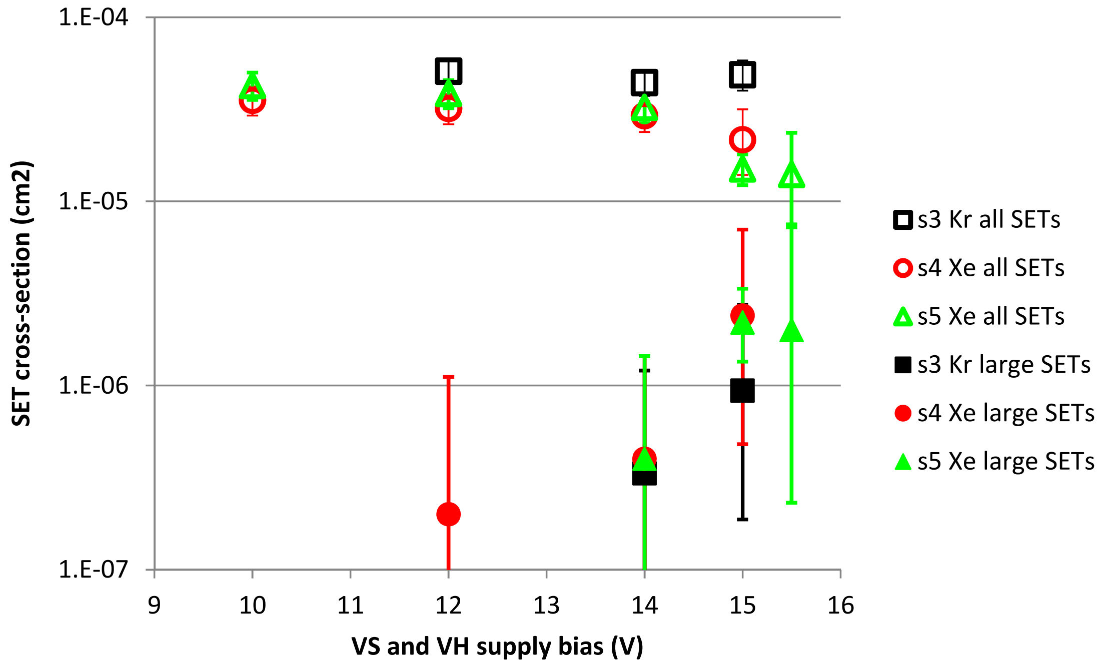

Figure 10: Cross-section for all (narrow and large) OUTA SETs (open symbols) and large only OUTA SETs (full symbols) for samples s3, s4, s5 with Kr (roll angle -60°) or Xe (normal incidence) ions, versus the ISL7457 bias (=VS=VH). The error bars are plotted according to [AD1], i.e 95% confidence level 10% fluence uncertainty)

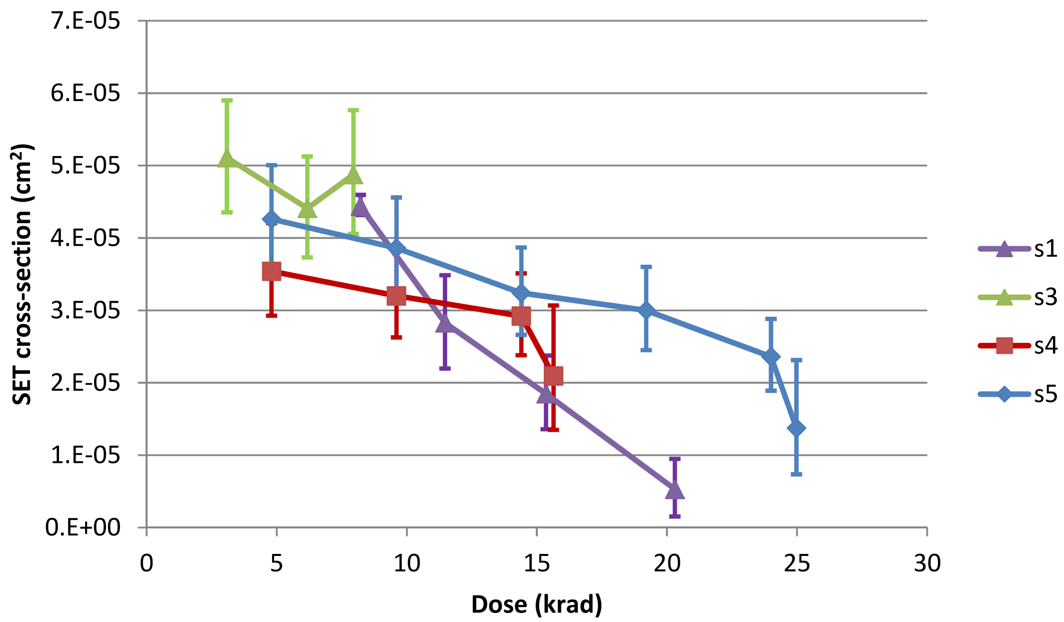

Figure 11: SET cross-section for all (narrow and large) OUTA SETs versus the total ionising dose deposited by heavy ions, for samples s1, s3, s4, s5.

8 CONCLUSION

The SEB sensitivity appears to be located in the protection structures attached to the device outputs , as observed for three of the irradiated samples. These protection structures are presumably off-state (gate grounded) MOS transistors. They fail by burn-out under heavy ion irradiation when the output is in high state. For two of the samples the failure site could not be visually located, indicating that the failure damage is either too small or hidden by the upper layer of the back-end-of-line. The failure mode in the ISL7457/PROTO is different from the previous version of the device EL7457 for which failures were located in the power MOSFET.

The sensitive cross-section of all SETs, narrow and large, is consistent with the area of the protection structures attached to the high state outputs. This may in the future be confirmed with focused pulse laser or an ion microprobe. SEBs are linked to large SETs that start appearing at 12 V bias voltage and exponentially increase with increasing device supply voltage. It is therefore recommended to use the ISL7457 device biased below 12 V to avoid SEBs.

The purpose of this test was to determine the failure mode of the ISL7457 device. For a more accurate analysis of its failure rate in space, it is recommended to perform a SEE test on the flight lot.

The following safe operating area is recommended:

- Threshold LET 45 MeVcm^2/mg, corresponding to run2 (Kr, LET 32 MeVcm^2/mg tilted at 45°) for which no burnout was observed up to a fluence of 8E6 ions/cm^2.
- Cross-section 2E-6 cm^2, which is the worst-case observed (run1) with a fluence of failure of 5E5 ions/cm^2 under Xe at LET 60 MeVcm^2/mg.

With these parameters, the analysis in [RD7] found a 1:14000 probability of failure for the 3.5 year CHEOPS mission.

9 APPENDIX 1: IRRADIATION TEST RUNS

Date: 12 Nov. 2014, RADEF

Beam: Xe 1217 MeV, range 89 µm, LET 60 $MeVcm^2/mg$
DUT in place: ISL7457SRHF PROTO sample s2

Run	Start	Angle	Effective LET ($MeVcm^2/mg$)	TID (krad)	VS & VH (V)	IS (mA)	IH (µA)	Irrad time (s)	Fluence (cm^{-2})	nb of all SETs	All SET cross-section (cm^2)	nb of large SETs	All SET cross-section (cm^2)
1	11:30	0°	60	1.5	15 V	1.56 mA	27 µA	183	1.56E+6	--	--	--	--

Sample s2 broken during run1 at about 5E5 Xe $ions/cm^2$.
The number of SETs were not registered during this first run.

Beam: Kr 768 MeV, range 94 µm, LET 32.1 MeVcm2/mg
DUT in place: ISL7457SRHF PROTO sample s1
Investigation of Tilt and Roll angles under Kr irradiation.
Note that the cumulated dose is calculated on the normal incidence LET:
Dose [krad] = Fluence [cm^{-2}] × LET [$MeVcm^2/mg$] × $1.6\times10^{-5}\times10^{-3}$ (see [AD1])

Run	Start	Angle	Effective LET ($MeVcm^2/mg$)	TID (krad)	VS & VH (V)	IS (mA)	IH (µA)	Irrad time (s)	Fluence (cm^{-2})	nb of all SETs	All SET cross-section (cm^2)	nb of large SETs	Large SET cross-section (cm^2)
2	11:50	Tilt 45°	45.4	4.11	15 V	1.5 mA	30 µA	626	8.00E+6	27	3.38E-6	--	--
3	12:00	Tilt 60°	64.2	8.22	15 V	1.5 mA	30 µA	584	8.00E+6	355	4.44E-5	--	--
4	12:15	Tilt -60°	64.2	11.47	15 V	1.5 mA	30 µA	408	6.33E+6	179	2.83E-5	13	2.05E-6
5-6	Dummy runs			12.27				119	1.55E+6				
7	12:45	Roll 60	64.2	15.35	15 V	1.5 mA	30 µA	467	6.01E+6	111	1.85E-5	21	3.49E-6
8	13:40	Roll -60	64.2	20.30	15 V	1.5 mA	30 µA	63	9.64E+6	51	5.29E-6	1	1.04E-7

Sample s1 broken during run8 at about 9E6 Kr $ions/cm^2$.
When the sample breaks, VH supply current goes to the compliance (10mA), but VS supply current stays at about 1.5mA.

Beam: Kr 768 MeV, range 94 µm, LET 32.1 MeVcm2/mg
DUT in place: ISL7457SRHF PROTO sample s3

Run	Start	Angle	Effective LET (MeVcm²/mg)	TID (krad)	VS & VH (V)	IS (mA)	IH (µA)	Irrad time (s)	Fluence (cm⁻²)	nb of all SETs	All SET cross-section (cm²)	nb of large SETs	Large SET cross-section (cm²)
9	14:05	Roll - 60°	64.2	3.09	12 V	1.15 mA	24 µA	354	6.01E+6	307	5.11E-5	0	0.00E+00
10	14:18	Roll - 60°	64.2	6.17	14 V	1.41 mA	28 µA	378	6.01E+6	265	4.41E-5	2	1.33E-06
11	14:26	Roll - 60°	64.2	7.95	15 V	1.54 mA	30 µA	229	3.45E+6	156	4.88E-5	3	3.75E-06

Sample s3 broken during run15 at about 3.2E6 Kr ions/cm².

Beam: Xe 1217 MeV, range 89 µm, LET 60 MeVcm²/mg
DUT in place: ISL7457SRHF PROTO sample s4

Run	Start	Angle	Eff. LET (MeVcm²/mg)	TID (krad)	VS & VH (V)	IS (mA)	IH (µA)	Irrad time (s)	Fluence (cm⁻²)	nb of all SETs	All SET cross-section (cm²)	nb of large SETs	Large SET cross-section (cm²)
12	15:17	0°	60	4.80	10 V	0.93 mA	20 µA	223	5.00E+6	177	3.54E-5	0	0.00E+00
13	15:22	0°	60	9.60	12 V	1.2 mA	24 µA	249	5.00E+6	160	3.20E-5	1	8.00E-07
14	15:27	0°	60	14.40	14 V	1.47 mA	28 µA	200	5.00E+6	146	2.92E-5	2	1.60E-06
15	15:35	0°	60	15.64	15 V	1.59 mA	30 µA	53	1.29E+6	27	2.09E-5	3	9.60E-06

Sample s4 broken during run15 at about 1.25E6 Xe ions/cm².

Beam: Xe 1217 MeV, range 89 µm, LET 60 MeVcm²/mg
DUT in place: ISL7457SRHF PROTO sample s5

Run	Start	Angle	Eff. LET (MeVcm²/mg)	TID (krad)	VS & VH (V)	IS (mA)	IH (µA)	Irrad time (s)	Fluence (cm⁻²)	nb of all SETs	All SET cross-section (cm²)	nb of large SETs	Large SET cross-section (cm²)
16	15:53	0°	60	4.80	10 V	0.87 mA	20 µA	276	5.00E+6	213	4.26E-5	0	0.00E+00
17	16:00	0°	60	9.60	12 V	1.12 mA	24 µA	250	5.00E+6	193	3.86E-5	0	0.00E+00
18	16:06	0°	60	14.40	14 V	1.38 mA	28 µA	236	5.00E+6	162	3.24E-5	2	1.60E-06
19	16:13	0°	60	19.20	15 V	1.51 mA	30 µA	237	5.00E+6	150	3.00E-5	13	1.04E-05
20	16:35	0°	60	24.00	15 V	1.5 mA	30 µA	266	5.00E+6	118	2.36E-5	9	7.20E-06
21	16:49	0°	60	24.98	15.5 V	1.57 mA	31 µA	54	1.02E+6	14	1.37E-5	0	8.00E-06

Sample s5 broken during run15 at about 1.0E6 Xe ions/cm².

10 APPENDIX 2: MICROSCOPE VIEW OF THE FAILURE SPOT

Sample 1

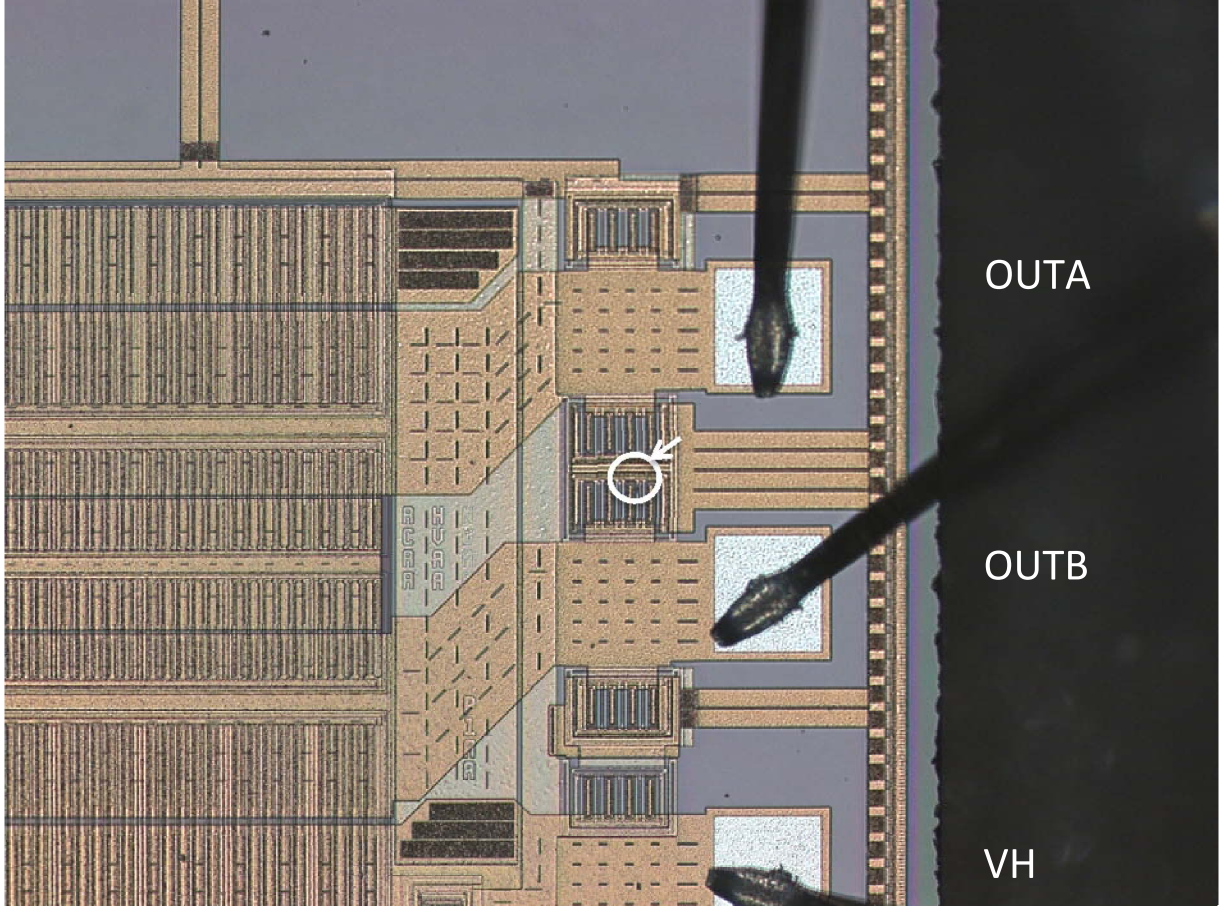

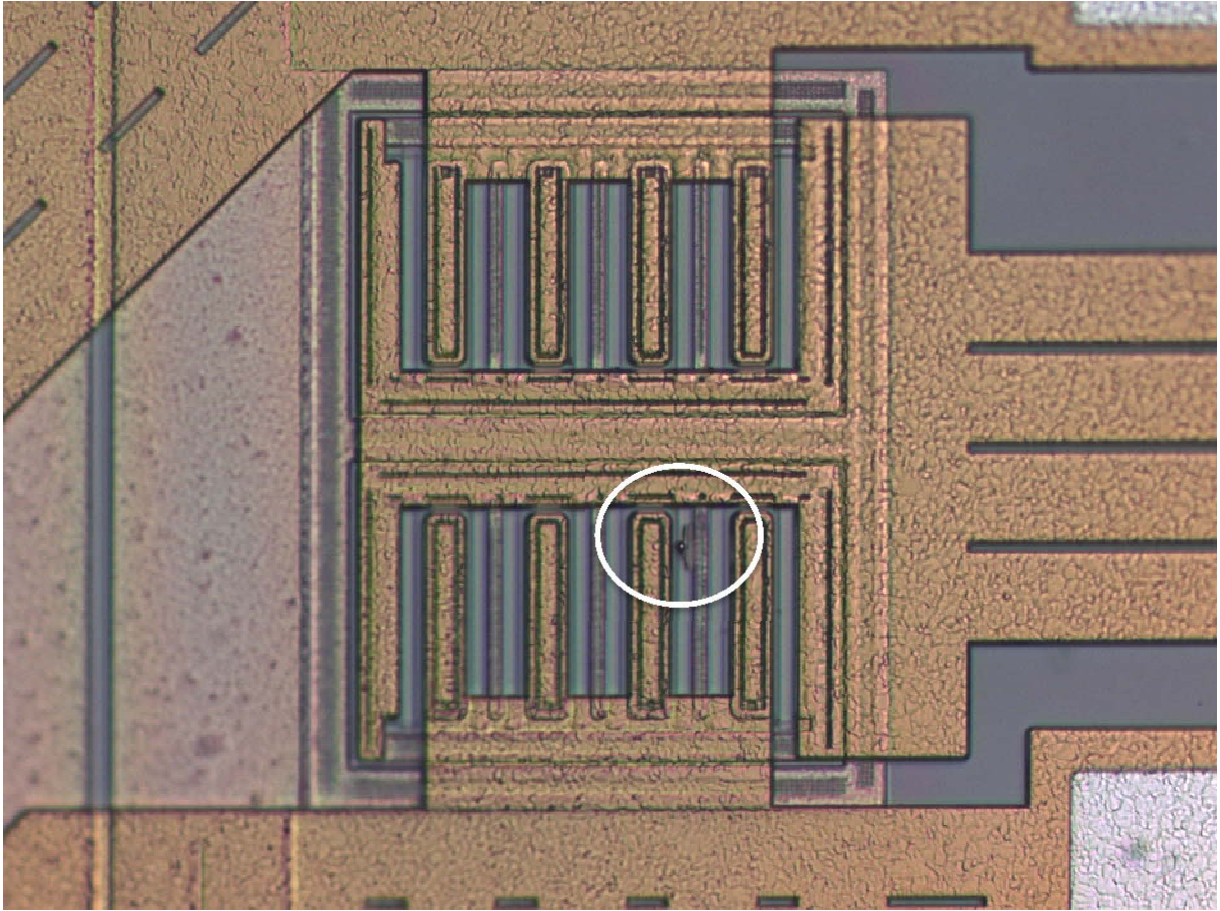

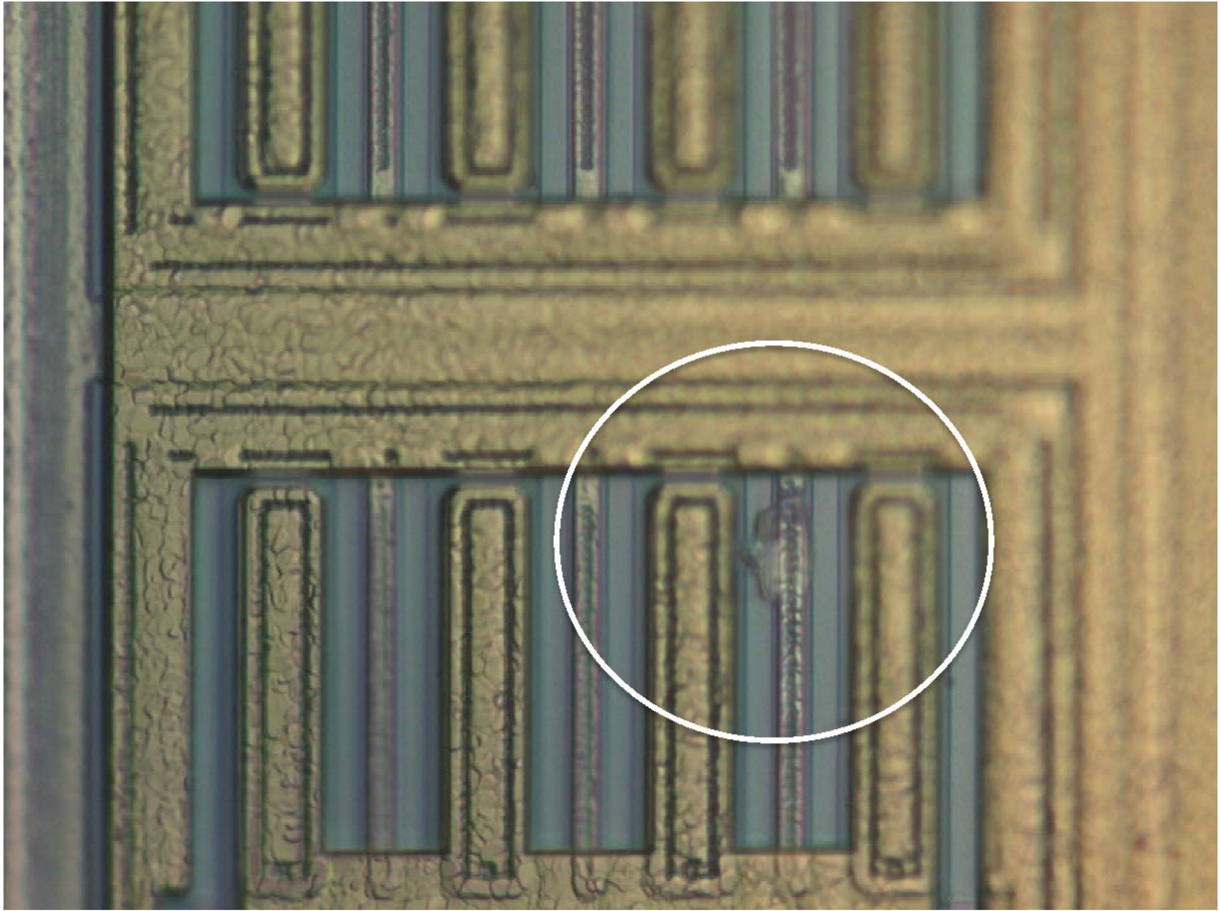

Sample 3

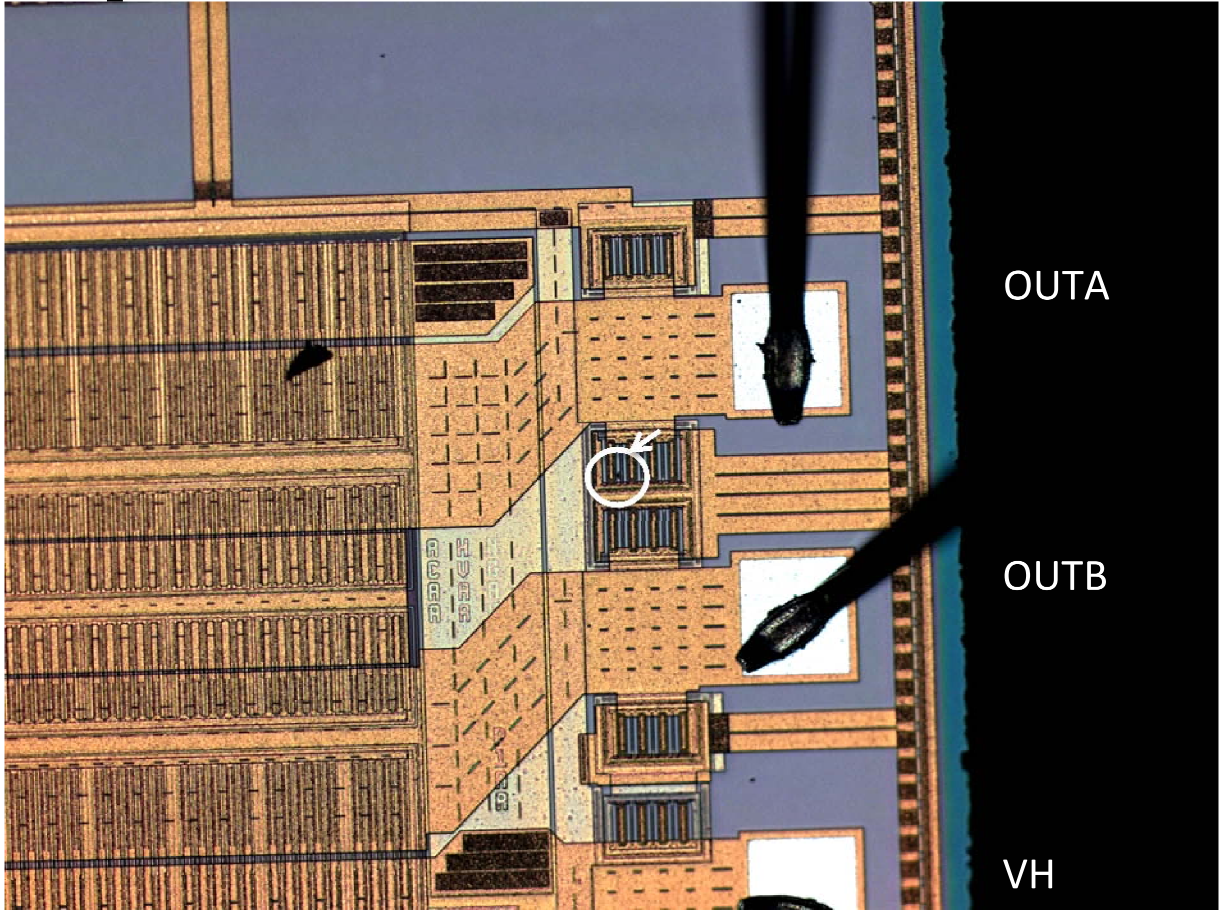

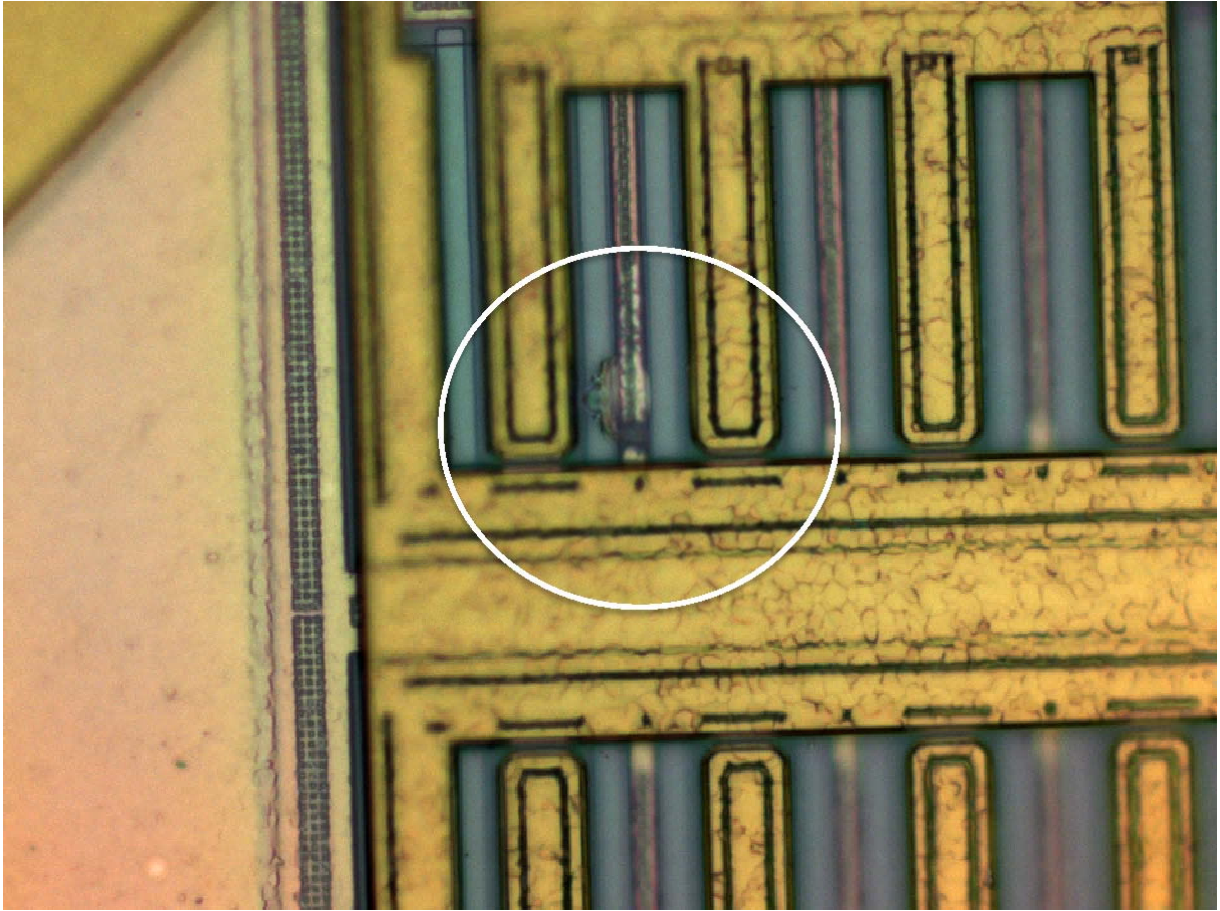

Sample 5